Observation of subkelvin superconductivity in Cd_{3}As_{2} thin films

A. V. Suslov, A. B. Davydov, L. N. Oveshnikov, L. A. Morgun, K. I. Kugel, V. S. Zakhvalinskii, E. A. Pilyuk, A. V. Kochura, A. P. Kuzmenko, V. M. Pudalov, and B. A. Aronzon

Phys. Rev. B **99**, 094512 — Published 14 March 2019

DOI: 10.1103/PhysRevB.99.094512

Observation of sub-kelvin superconductivity in Cd_3As_2 thin films

A.V. Suslov[1], A.B. Davydov[2], L.N. Oveshnikov[3,2,*], L.A. Morgun[2,4], K.I. Kugel[5,4], V.S. Zakhvalinskii[6], E.A. Pilyuk[6], A.V. Kochura[7], A.P. Kuzmenko[7], V.M. Pudalov[2,4], B.A. Aronzon[3,2]

[1]*National High Magnetic Field Laboratory, Tallahassee, Florida, 32310 USA*
[2]*P. N. Lebedev Physical Institute, Russian Academy of Sciences, Moscow, 119991 Russia*
[3]*National Research Center "Kurchatov Institute", Moscow, 123182 Russia*
[4]*National Research University Higher School of Economics, Moscow, 101000 Russia*
[5]*Institute for Theoretical and Applied Electrodynamics, Russian Academy of Sciences, Moscow, 125412 Russia*
[6]*Belgorod National Research University, Belgorod, 308015 Russia*
[7]*South-West State University, Kursk, 305040 Russia*

(Dated: February 13, 2019)

We report the first experimental observation of superconductivity in Cd_3As_2 thin films without application of external pressure. The films under study were synthesized by magnetron sputtering. Surface studies suggest that the observed transport characteristics are related to the polycrystalline continuous part of investigated films with homogeneous distribution of elements and the Cd-to-As ratio close to stoichiometric Cd_3As_2. The latter is also supported by Raman spectra of the studied films where two pronounced peaks inherent to Cd_3As_2 were observed. Obtained X-ray diffraction patterns for studied films also corresponds to the Cd_3As_2 lattice. The formation of superconducting phase in films under study is confirmed by the characteristic behavior of temperature and magnetic field dependence of samples resistivity, as well as by the presence of pronounced zero-resistance plateaux in dV/dI characteristics. The corresponding $H_c - T_c$ plots reveal a clearly pronounced linear behavior within the intermediate temperature range, similar to that observed for bulk Cd_3As_2 and Bi_2Se_3 films under pressure, suggesting the possibility of nontrivial pairing in the films under investigation. We discuss a possible role of sample inhomogeneities and crystal strains in the observed phenomena.

I. INTRODUCTION

Weyl and Dirac semimetals (WSM and DSM) currently attract wide interest related to the existence of Dirac nodes in their electron spectrum and related nontrivial topological characteristics of both bulk and surface states[1–3]. A special attention is drawn to the Cd_3As_2 compound, which proved to be air-stable, unlike some other DSM materials[4–8]. This compound is known and has been studied for quite a long time[9–12]. Nevertheless, it is still very popular since the Dirac nodes of this semimetal are protected by the crystal symmetry and the electron states exhibit interesting topological properties, such as spin-momentum locking. Due to the high symmetry, DSM materials can undergo transitions to other topological phases (e.g. WSM) as a result of breaking certain symmetries or applying some external factors.

The existence of topologically protected electron states gives a new impetus to the problem of topological superconductivity (TSC) being discussed for a long time[13–15]. In particular, Sato *et al.*[16,17] performed a theoretical analysis of the possible types of superconducting (SC) pairing in the systems of Cd_3As_2 type, including topologically nontrivial ones. Basically, the existence of nontrivial pairing potential (leading to the emergence of triplet Cooper pairs) should induce the formation of Majorana modes at the surface of the crystal, which can be used in the fault-tolerant quantum computing[14]. The SC phase emergence in Cd_3As_2 was reported for bulk crystals[18], however, it was observed at pressures above the structural transition from the tetragonal to trigonal phase. While theoretical works suggest the stabilization of TSC phase upon such symmetry lowering[16,17], such transition also implies appearance of the gap at Dirac nodes, thus, suppressing the DSM phase. Additional indications of the SC phase in Cd_3As_2 were also observed in the point-contact spectroscopy experiments and attributed to the local crystal distortions under point-contact[19,20]. It is important to note, that up to now, all indications of the SC phase emergence in Cd_3As_2 were related either to the pressure-induced structural changes or to the proximity effect with the conventional s-wave SC[21–23].

Recent studies of Cd_3As_2 thin films outlined their specific features. The observation of quantum Hall state[24,25] and consecutive analysis of magnetoresistance of Cd_3As_2 films suggest the occurrence of Weyl orbits related to the surface states below some critical thickness[26,27]. Thus, superconducting Cd_3As_2 thin film with nontrivial pairing (TSC state) should yield surface Majorana modes, which, however, can be modified (in comparison to the bulk crystal[16]) due to interaction of opposite surfaces.

In the previous studies bulk Cd_3As_2 has not exhibited any indications of superconductivity except that arising at extremely high pressure. In contrast to this, we have observed superconductivity in Cd_3As_2 thin films without external compression. We argue that the observed phenomena cannot be related to any parasitic effects and it have certain similarities to the previously observed SC in Cd_3As_2 under pressure[18], suggesting the possible presence of nontrivial pairing in the studied films.

II. METHODS

The films under study were deposited by high-frequency magnetron nonreactive sputtering, performed with nominal radiation power of 10 W in the argon atmosphere with residual pressure of 0.7 Pa. Single crystals of Cd_3As_2 used for sputtering were grown by vapor phase deposition from high-purity initial components. In this paper, we present the results for three films, shaped into Hall bar geometry with a mm-scale conduction channel. Samples A and C were deposited onto polished p-Si substrates ($\rho_{sub} = 2\ \Omega \cdot$ cm) with native oxide layer, sample B was deposited onto Al_2O_3 substrate. During the deposition, the substrates were kept at room temperature. Deposition time for samples A and C was 20 min, for sample B – 40 min.

The initial surface studies of the grown films were conducted using the scanning electron microscope (SEM) JSM-6610LV (Jeol, Japan) with the additional X-Max^N module (Oxford Instruments, UK) for energy-dispersive X-ray spectroscopy (EDXS). For imaging, we used detectors for secondary and backscattered electrons. The additional studies were performed using atomic-force microscope (AFM) SmartSPM 1000 (AIST NT, USA). Raman spectra were recorded at room temperature using combined scanning probe microscopy system with the confocal fluorescence spectrometer and Raman spectrometer OmegaScope^{TM} (AIST NT, USA). For excitation we used a laser with 532 nm wavelength, power of 50 mW, and the focused light spot at the sample surface of about 500 nm. The spectral resolution was 0.8 cm^{-1}.

The X-ray diffraction (XRD) patterns of studied samples were obtained using the GBC EMMA analyser (GBC Scientific Equipment, Australia) with Cu radiation source ($\lambda = 1.54184$ Å). Due to samples geometry obtained XRD data also contain pronounced peaks related to the aluminium sample holder.

To eliminate all uncertainties related to the experimental artefacts in measurements of the transport properties of the samples, we used two different setups. Samples A and B were studied using a cryogen-free dilution refrigerator BF-LD250 with a 1 Tesla magnet (BlueFors, Finland) at the Lebedev Shared Facility Center, Moscow, Russian Federation. Those experiments were performed by the conventional low-frequency (7.142 Hz) lock-in four-probe method with measurement currents (of the order of 100 nA) considerably lower than critical values obtained for studied films. Sample C was studied using a 20 Tesla superconducting magnet with a dilution refrigerator (SCM1) at the National High Magnetic Field Laboratory (NHMFL), Tallahassee, Florida, USA. There a Model 372 ac resistance bridge with a preamp 3708 (Lake Shore Cryotronics, Inc., USA) was used for magnetoresistance testing by the four-probe method at current 316 nA. Measurements of the differential resistance dV/dI were performed utilizing a current source Model 6221 and a nanovoltmeter Model 2182A (Tektronix, Inc., USA).

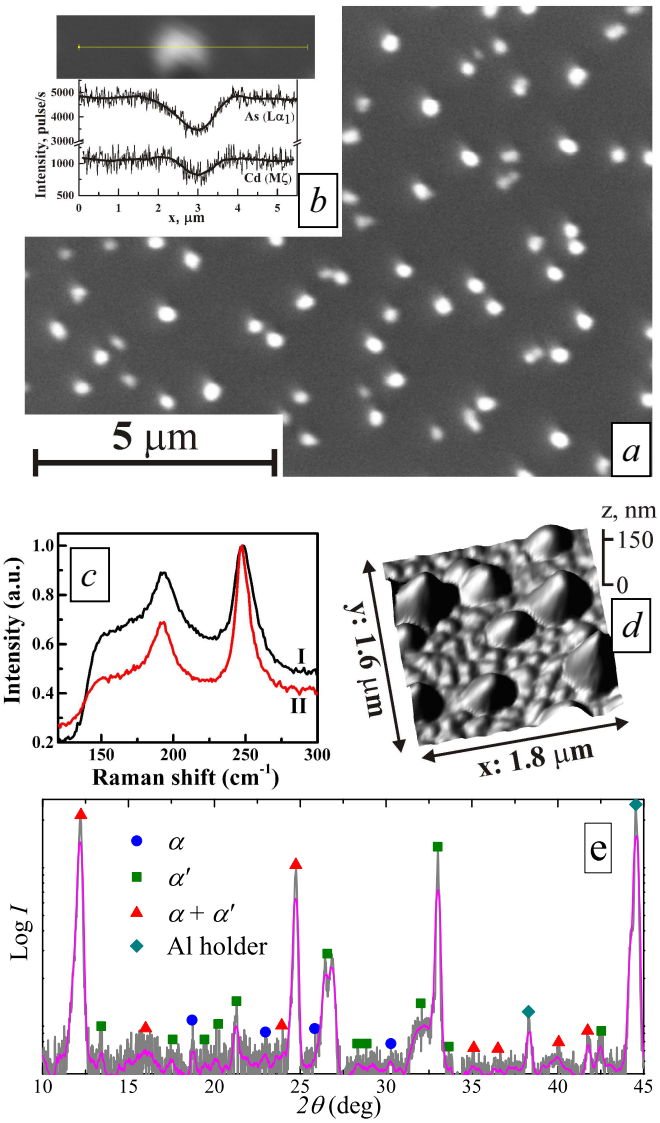

FIG. 1. (a) SEM image of the sample C surface. Light regions correspond to large grains at the surface of continuous films. (b) EDX scan: distribution of the Cd- and As-related peaks amplitudes within 1D scan across a surface grain as illustrated above. Corresponding amplitudes decrease in the surface grain area due to "shadowing" effect related to 3D shape of a surface grain. The Cd-to-As ratio within the whole scanning area is close to stoichiometric Cd_3As_2. (c) Raman spectra for sample C (I) and reference Cd_3As_2 single crystal (II). (d) 3D visualization of the AFM image of the surface of sample C. (e) XRD pattern for sample A (magenta line - smoothed data). Obtained pattern corresponds to α and α' modifications of the Cd_3As_2 lattice (see text).

III. EXPERIMENTAL RESULTS

SEM images of the studied films reveal similar surface morphology. As one can see in Fig. 1a, there are large grains at the surface of continuous film. The presence of such hemispherical grains corresponds to the island-type growth process of the film, which is quite common

for various methods of physical deposition. These grains have typical sizes of about 100–300 nm, while the distances between them are substantially larger. The latter suggests the absence of such grain overlapping, implying that transport properties are determined by the continuous part of the film located beneath them. The EDX mapping reveals a homogeneous distribution of components (Fig. 1b), implying that transport characteristics of the film are related solely to the Cd-As binary system. The EDXS demonstrates that at μm scale the Cd-to-As ratio is constant and close to the stoichiometric Cd_3As_2 within the 2% accuracy (according to a quantitative analysis of the EDX spectra, not provided in this article). The presence of Cd_3As_2 phase is also supported by the Raman spectroscopy results. A typical Raman spectrum for studied films is shown in Fig. 1c (curve I). As a reference, we also provide the Raman spectrum for Cd_3As_2 single crystal used as a target for sputtering (curve II). Earlier, it was shown that the presence of two main peaks around 200 cm^{-1} and 250 cm^{-1} is a characteristic feature of Raman spectra for Cd_3As_2 nanocrystallites[28] and thin films[29] measured at room temperature using unpolarized light. The obtained AFM images show that the surface regions between large grains are formed by smaller (about 40-50 nm) overlapping grains (Fig. 1d), suggesting the polycrystalline structure of continuous part of the film. The thickness of studied films determined by AFM is 40–50 nm for samples A and C, and about 80 nm for sample B.

While almost all theoretical considerations of Cd_3As_2 refer solely to single crystals, there is no profound arguments that the DSM phase will be inevitably absent in a polycrystalline sample, since the main features of the band structures in solids are usually formed at the scale of several lattice constants. Obviously, when the crystallite size is reduced down to nm-scale, the quantum size effect can substantially alter the band structure. Although there is no accurate estimation of nanocrystallite critical size, below which the DSM phase vanishes, typical Cd_3As_2 polycrystals are commonly used for the search of nontrivial topological features (e.g. the realization of TSC state[20]).

The structure of studied films was also investigated using XRD. The corresponding XRD pattern for sample A is shown in Fig. 1e. Except for two peaks related to the sample holder, the obtained patterns, including low-intensity peaks, can be interpreted in terms of α (sp.gr. $I4_1/acd$, $a = 12.6461$ Å, $b = 25.4378$ Å) and α' (sp.gr. $P4_2/nbc$, $a = 12.6848$ Å, $b = 25.4887$ Å) modifications of the Cd_3As_2 lattice[30]. The main difficulty is that both α and α' modifications have tetragonal lattices with very close unit cell parameters. Thus, the corresponding diffraction peaks are very close to each other, and several of them are simply indistinguishable (marked as $\alpha+\alpha'$ in Fig. 1e). While the appearance of the α'-Cd_3As_2 phase in our case can be related to the fast cooling of the film during synthesis process[31], the existence of two polymorphic phases agrees well with the polycrystalline structure

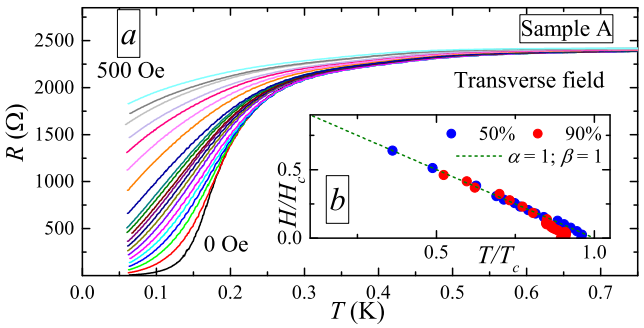

FIG. 2. (a) Temperature dependence of resistivity for sample A at various transverse magnetic fields. (b) Corresponding $H_c - T_c$ diagrams for SC transition estimated as a resistance drop to 50% (midpoint) and 90% of the normal value. Fitting of experimental data by Eq. (1) is shown by the dashed line.

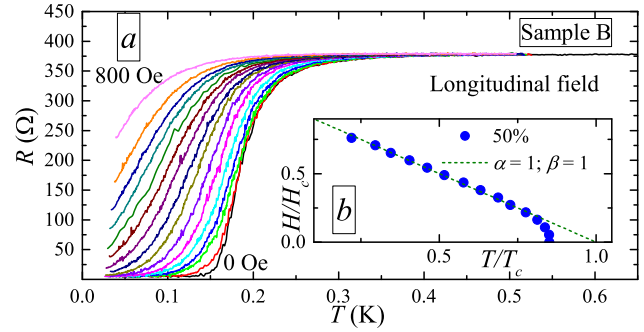

FIG. 3. (a) Temperature dependence of resistivity for sample B at various longitudinal magnetic fields. (b) Corresponding $H_c - T_c$ diagrams for SC transition (midpoint). Fitting of experimental data by Eq. (1) is shown by the dashed line.

of the studied films. A very subtle difference between α and α' lattices suggests that the corresponding electron spectra are also very close, implying the existence of the DSM phase in both cases. We should also mention that the most intense diffraction peak at $2\theta \approx 12°$ corresponds to the (112) plane and suggests a partial orientation of crystallites in the film. The width of this peak corresponds to the mean crystallite size of about 35 nm (estimated using standard Debye-Scherrer equation with shape factor of 0.9), which agrees well with the sizes of grains in continuous part of the film determined by AFM (see Fig. 1d).

Transport measurements of the studied films reveal a clearly pronounced SC transition below 0.5 K. In Fig. 2a, we show the temperature dependence of resistivity for sample A at various values of the transverse magnetic field. As one can see, there is a distinct resistance drop (to almost zero value, of the order of measurement noise level) that shifts to the lower temperatures upon increasing magnetic field, which supports the assumption of SC phase emergence. Sample B demonstrates analogous behavior (see Fig. 3a). The actual transition regions are rather broad, which agrees well with the polycrystalline structure of the films.

The dV/dI characteristics (not to be confused with tunnel spectra) for sample C measured at various tem-

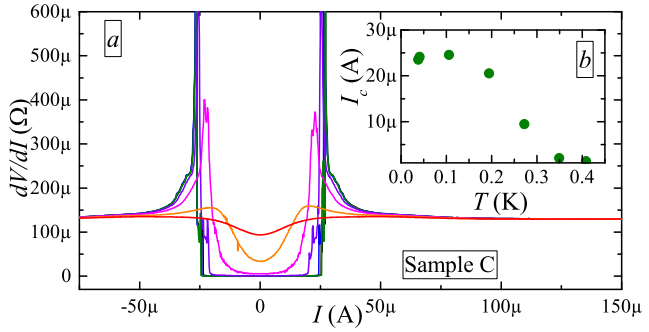

FIG. 4. (a) Differential resistance for sample C at various temperatures. (b) Corresponding temperature dependence of critical current, I_c.

peratures clearly demonstrate zero-resistance plateaux (Fig. 4a). The critical current values, I_c, decrease as the temperature approaches T_c (Fig. 4b). However, at the lowest temperatures I_c appears to be temperature-independent. The magnetoresistivity (MR) of sample C exhibits typical features of field induced SC-to-normal state transition (Figs. 5a and 5b). As the temperature increases, the zero-field resistivity becomes higher, although the shape of MR curves remains similar. We clearly observe the anisotropy of critical magnetic field: H_c values for longitudinal field are considerably higher than those for transverse field, which is common for thin SC films.

Assuming that H_c corresponds to the 50% resistance drop of its normal value (midpoint), we obtained $H_c - T_c$ diagrams for the studied samples (Figs. 2b, 3b and 5c). To characterize the observed SC state, we applied the conventional formula describing the decrease in the critical magnetic field, H_c, upon increasing the temperature below critical value T_c:

$$H(T) = H_c(0) \cdot \left(1 - \left(\frac{T}{T_c}\right)^{\alpha}\right)^{\beta}. \qquad (1)$$

Here, $\alpha = 2; \beta = 1$ corresponds to the common Bardeen-Cooper-Schrieffer (BCS) theory at low temperatures, while the Ginzburg-Landau (G-L) theory suggests $\alpha = 1; \beta = 1$ to describe the temperature dependence of upper critical field, H_{c2}, in type-II SC close to T_c. It is important to note that the presented $H_c - T_c$ diagrams for studied samples cannot be approximated well by Eq. (1) with $\alpha = 2; \beta = 1$. However, in the intermediate temperature range, the obtained diagrams can be effectively described with linear function ($\alpha = 1; \beta = 1$) as it is shown in the corresponding figures. The deviations from this line in the vicinity of T_c (samples A and B) and low-temperature saturation (sample C) requires additional investigation and can be related to the polycrystallinity of studied films. Nevertheless, the overall behavior of $H_c - T_c$ diagrams for transverse and longitudinal magnetic fields is essentially the same. It is worth mentioning that there is no qualitative difference if we ascribe T_c and H_c to the 90% value of normal state resistivity (see Fig. 2b).

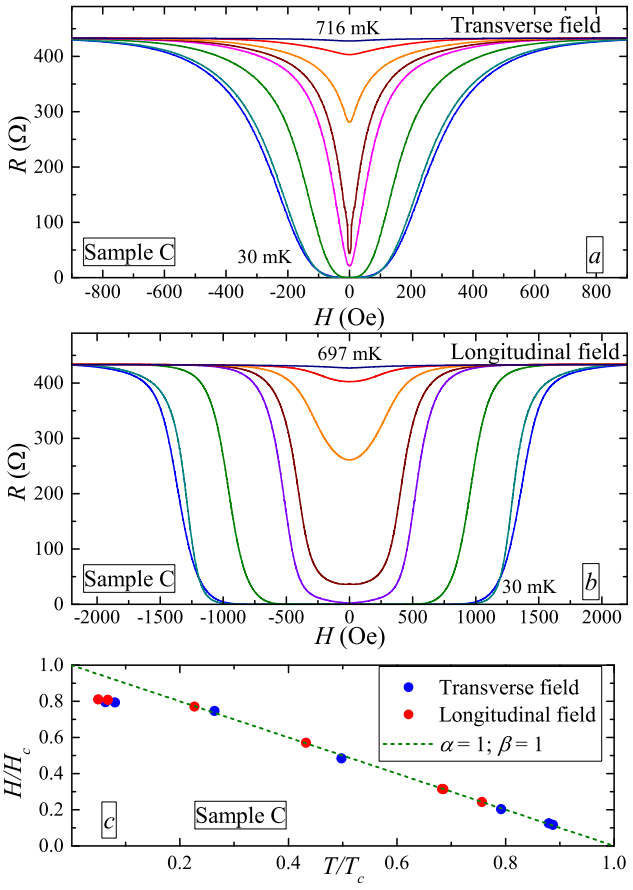

FIG. 5. Low-field magnetoresistivity of sample C at various temperatures at (a) transverse and (b) longitudinal magnetic fields. (c) Corresponding $H_c - T_c$ diagrams for the SC transition.

IV. DISCUSSION

The absence of elemental segregation (confirmed by EDXS results) implies that the observed SC phase cannot be attributed to the elemental Cd, which is a classical SC with $T_c = 0.56$ K and $H_c \approx 30$ Oe[32,33] (also, the H_c values for studied films are substantially higher, e.g. for sample A the transverse $H_c \approx 350$ Oe). Additionally, due to relatively large sizes of conducting channel, the observed SC cannot be related to an influence of the contact regions. Thus, we can conclude that the observed SC phase emerges within Cd-As binary system with the elemental ratio close to stoichiometric Cd_3As_2 compound. Alongside with the observed features in XRD patterns and Raman spectra (inherent to the Cd_3As_2 crystal phase), this suggests a possible coexistence of SC and DSM phase within studied films, which can support the formation of surface Majorana modes[16,17].

Originally, the G-L theory describes SC in the vicinity of T_c. However, fairly often it is applied in a much broader temperature range[34]. In our study, application of the G-L theory implies that transverse H_c values extrapolated to zero temperature can be used for the estimation of coherence length ξ ($H_c(0) = \phi_0/(2\pi\xi^2)$, ϕ_0

- magnetic flux quantum). For sample C, we obtain $\xi \approx 100$ nm (for the midpoint H_c value), which is twice as high as the film thickness. The latter suggests that the observed SC should be two-dimensional, and the corresponding $H_c - T_c$ diagram for longitudinal field should follow Eq. (1) with $\alpha = 1; \beta = 1/2$[35]. The temperature range, where this type of $H_c - T_c$ correlation should be observed, depends on various parameters of the film[36]. Thus, the absence of such behavior for studied films suggest that it may be very narrow. On the other hand, the isotropic linear character of $H_c(T)$ dependeces may also indicate that some additional effects are relevant in our case. A more general approach[37] suggests that linear $H_c - T_c$ relation in the wide temperature range can be observed for systems with strong pairing interaction. According to the phase diagram of SC in Cd_3As_2[15,17], the type of pairing potential (even- or odd-parity) depends not on the integral strength of e–e attraction, but rather on the relation between intra- and inter-orbital components. However, in the studies of pressure-induced SC in Cd_3As_2[18] and Bi_2Se_3[38,39], the linear character of $H_c - T_c$ diagram (alongside with the saturation of pressure dependence of T_c) was considered as a signature of nontrivial pairing (of odd-parity). Similarly, in our case the obtained $H_c - T_c$ diagrams with pronounced linear behavior also may indicate the presence of odd-parity pairing potential in the studied films. However, to verify the topological nature of the observed SC, one needs to perform a set of various experiments[15], which are technologically challenging in our case and require further studies.

From the conventional point of view, the SC phase emergence in our case is favored due to high electron densities (the Hall concentrations for studied films are about 8–12·10^{18} cm^{-3}). It implies that the Fermi level lies substantially higher than the Lifshitz transition of pristine Cd_3As_2 single crystals, meaning that transport features of DSM phase might be damped, although the band structure may preserve the nonzero Berry curvature[40]. Nevertheless, the substantial increase in the electron density in topological materials always precedes the SC phase emergence, which, however, is argued to sustain topological features[18,38,39]. Considering the fact that high quality Cd_3As_2 single crystalline films studied in similar temperature range did not exhibit any SC transition[27], we assume that the SC phase in our case results from possible crystal structure distortions.

Knowing that intrinsic SC emergence in Cd_3As_2 is induced by pressure[18–20], we also tend to assume that the observed SC can be affected by strain existing within a film (e.g. due to polycrystalline character). Due to relatively small thickness of the studied films, such strain can be also related to the difference of the coefficients of thermal expansion (CTE) of the substrate and the film. At room temperature, Cd_3As_2 is characterized by large CTE value of about $\alpha_{CdAs} \sim 11.8 - 12.4 \cdot 10^{-6}\,\mathrm{K}^{-1}$. It decreases with the temperature as it is for normal metal[31]. Al_2O_3 has anisotropic CTE (from $\alpha_{\parallel} = 6.7 \cdot 10^{-6}\,\mathrm{K}^{-1}$ to $\alpha_{\perp} = 5.0 \cdot 10^{-6}\,\mathrm{K}^{-1}$) at room temperature[41]. Si has smaller CTE at room temperatures ($\alpha_{Si} = 2.54 \cdot 10^{-6}\,\mathrm{K}^{-1}$) and exhibits even negative values at lower temperatures, 20–110 K[42]. Thus, as the temperature decreases, the Al_2O_3 substrate contracts less, and the Si substrate contracts even much less than the Cd_3As_2 film. As a result, studied samples should experience the tensile strain in the temperature range under study. We did not manage to find either the experimental or theoretical studies of Cd_3As_2 phase diagram under negative pressures, making it hard to predict the effect of such strain. We observed close values of $T_c \approx 190$ mK (midpoint) for samples A (40 nm film on a Si substrate) and B (80 nm film on a Al_2O_3 substrate) with substantially different width of SC transition. Moreover, preliminary studies of films deposited at the same conditions on the fused quartz substrates (with $\alpha \ll \alpha_{Si}$) revealed the absence of SC transition down to 40 mK. Thus, it is clear that the substrate strongly affects the emergent SC state in studied films. However, to elucidate all relevant effects, an additional investigation is highly needed.

We would like to emphasize that the observation of zero resistance and consistent character of the $I_c(T)$ and $H_c(T)$ dependences implies that SC state is attributed to the whole sample. Due to polycrystalline character of studied films the exact structure of grain boundaries can affect the emergent SC (e.g. by changing the I_c values), which is common for many conventional SC. However, to relate the observed SC solely to the grain boundaries, one needs to assume that these boundaries have a very specific structure, which is highly unlikely to occur in a real sample.

It is important to note that the indications of surface SC in Cd_3As_2 single crystals was recently reported[43]. The apparent difference is that we observed zero resistance of the whole film, while the SC in corresponding crystals[43] results only in the 10% drop of surface resistance. Whereas this difference may be related to various reasons, the properties of Majorana modes in our case can be different from those of single DSM surface[17] due to Weyl orbit formation. However, as it was recently demonstrated in the Josephson junction experiments[23], to reveal any particular anomalies of the topological surface-mediated superconductivity, one needs to investigate corresponding phenomena within a broad range of Fermi energies, which strongly motivates further research of studied films.

V. CONCLUSIONS

In this article, we report the first experimental observation of superconductivity emergence in cadmium arsenide films without any applied pressure. The superconducting nature of the transition observed in $R(T)$ dependence is justified by differential resistance and magnetoresistivity measurements, providing temperature dependence of corresponding critical parameters (I_c and H_c). We argue

that the observed phenomena cannot be attributed to any parasitic effects such as elemental Cd segregation or any effects related to contact regions. The observed SC state is characterized by $H_c - T_c$ diagrams with a pronounced linear regions at intermediate temperatures for both the transverse and longitudinal magnetic fields. The deviations from overall linear dependence at low temperatures and close to T_c can be related to the polycrystallinity of studied films. Similar linear $H_c(T)$ dependence was considered as a signature of nontrivial pairing potential in bulk Cd_3As_2 and Bi_2Se_3 films under pressure. Theory suggests that such pairing potential should result in the formation of surface Majorana modes. Favored by high electron densities, the observed superconducting state can emerge due to distortion of the film crystal structure, which arises during the deposition procedure using the magnetron sputtering. We argue that this SC state can be affected by various strains arising in the films under study. We also note that similar films deposited on fused quartz substrates do not exhibit the superconducting state emergence down to 40 mK. Thus, it is possible to substantially affect the observed SC state. The latter indicates that the investigated systems might be a promising platform for studies of topological superconductivity.

Acknowledgements

The work was partially supported by the Russian Science Foundation, grant No. 17-12-01345. A portion of this work was performed at the National High Magnetic Field Laboratory, which is supported by the National Science Foundation Cooperative Agreement No. DMR-1644779 and the State of Florida. A portion of theoretical analysis, performed by V.M.P., was supported by Russian Foundation for Basic Research, grant No. 16-29-03330. We would like to thank K.V. Mitsen and O.M. Ivanenko for fruitful discussions and H. Baek and G. Jones for technical assistance at the NHMFL.

[1] N. P. Armitage, E. J. Mele, and A. Vishwanath, "Weyl and Dirac semimetals in three-dimensional solids," Rev. Mod. Phys. **90**, 015001 (2018).
[2] B. Yan and C. Felser, "Topological materials: Weyl semimetals," Annu. Rev. Condens. Matter Phys. **8**, 337 (2017).
[3] S. Wang, B.-C. Lin, A.-Q. Wang, D.-P. Yu, and Z.-M. Liao, "Quantum transport in Dirac and Weyl semimetals: a review," Adv. Phys. X **2**, 518 (2017).
[4] M. Neupane, S. Y. Xu, R. Sankar, N. Alidoust, G. Bian, C. Liu, I. Belopolski, T. R. Chang, H. T. Jeng, H. Lin, et al., "Observation of a three-dimensional topological Dirac semimetal phase in high-mobility Cd_3As_2," Nat. Commun. **5**, 3786 (2013).
[5] Z. K. Liu, J. Jiang, B. Zhou, Z. J. Wang, Y. Zhang, H. M. Weng, D. Prabhakaran, S. K. Mo, H. Peng, P. Dudin, et al., "A stable three-dimensional topological Dirac semimetal Cd_3As_2," Nat. Mater. **13**, 677 (2014).
[6] S. Jeon, B. B. Zhou, A. Gyenis, B. E. Feldman, I. Kimchi, A. C. Potter, Q. D. Gibson, R. J. Cava, A. Vishwanath, and A. Yazdani, "Landau quantization and quasiparticle interference in the three-dimensional Dirac semimetal Cd_3As_2," Nat. Mater. **13**, 677 (2014).
[7] S. Borisenko, Q. Gibson, D. Evtushinsky, V. Zabolotnyy, B. Büchner, and R. J. Cava, "Experimental Realization of a Three-Dimensional Dirac Semimetal," Phys. Rev. Lett. **113**, 027603 (2014).
[8] L. Lu, Z. Wang, D. Ye, L. Ran, L. Fu, J. D. Joannopoulos, and M. Soljačić, "Experimental observation of Weyl points," Science **349**, 622 (2015).
[9] J. J. Dubowski and D. F. Williams, "Pulsed laser evaporation of Cd_3As_2," Appl. Phys. Lett. **44**, 339 (1984).
[10] C. Weclewicz and L. Zdanowicz, "Transport properties of thin amorphous films of cadmium arsenide," Thin Solid Films **151**, 87 (1987).
[11] A. A. El-Shazly, H. Soliman, D. Abd El-Hady, and H. E. A. El-Sayed, "Transport properties of thin Cd_3As_2 polycrystalline films," Vacuum **47**, 45 (1996).
[12] B. Jarzabek, J. Weszka, , and J. Cisowski, "Distribution of electronic states in amorphous Cd-As thin films on the basis of optical measurements," J. Non-Cryst. Solids **333**, 206 (2004).
[13] L. A. Wray, S.-Y. Xu, Y. Xia, Y. S. Hor, D. Qian, A. V. Fedorov, H. Lin, A. Bansil, R. J. Cava, and M. Z. Hasan, "Observation of topological order in a superconducting doped topological insulator," Nat. Phys. **6**, 855 (2010).
[14] Y. Ando and L. Fu, "Topological crystalline insulators and topological superconductors: From concepts to materials," Annu.l Rev. Condens. Matter Phys. **6**, 361 (2015).
[15] M. Sato and Y. Ando, "Topological superconductors: a review," Rep. Prog. Phys. **80**, 076501 (2017).
[16] S. Kobayashi and M. Sato, "Topological Superconductivity in Dirac Semimetals," Phys. Rev. Lett. **115**, 187001 (2015).
[17] T. Hashimoto, S. Kobayashi, Y. Tanaka, and M. Sato, "Superconductivity in doped Dirac semimetals," Phys. Rev. B **94**, 014510 (2016).
[18] L. He, Y. Jia, S. Zhang, X. Hong, C. Jin, and S. Li, "Pressure-induced superconductivity in the three-dimensional topological Dirac semimetal Cd_3As_2," Npj Quant. Mater. **1**, 16014 (2016).
[19] H. Wang, H. Wang, H. Liu, H. Lu, W. Yang, S. Jia, X.-J. Liu, X. C. Xie, J. Wei, and J. Wang, "Observation of superconductivity induced by a point contact on 3D Dirac semimetal Cd_3As_2 crystals," Nat. Mater. **15**, 38 (2015).
[20] L. Aggarwal, A. Gaurav, G. S. Thakur, Z. Haque, A. K. Ganguli, and G. Sheet, "Unconventional superconductivity at mesoscopic point contacts on the 3D Dirac semimetal Cd_3As_2," Nat. Mater. **15**, 32 (2015).
[21] C.-Z. Li, C. Li, L.-X. Wang, S. Wang, Z.-M. Liao, A. Brinkman, and D.-P. Yu, "Bulk and surface states carried supercurrent in ballistic Nb-Dirac semimetal Cd_3As_2 nanowire-Nb junctions," Phys. Rev. B **97**, 115446 (2018).

[22] W. Yu, W. Pan, D. L. Medlin, M. A. Rodriguez, S. R. Lee, Z.-q. Bao, and F. Zhang, "π and 4π Josephson effects mediated by a Dirac semimetal," Phys. Rev. Lett. **120**, 177704 (2018).

[23] A.-Q. Wang, C.-Z. Li, C. Li, Z.-M. Liao, A. Brinkman, and D.-P. Yu, "4π-periodic supercurrent from surface states in Cd_3As_2 nanowire-based Josephson junctions," Phys. Rev. Lett. **121**, 237701 (2018).

[24] M. Uchida, Y. Nakazawa, S. Nishihaya, K. Akiba, M. Kriener, Y. Kozuka, A. Miyake, Y. Taguchi, M. Tokunaga, N. Nagaosa, et al., "Quantum Hall states observed in thin films of Dirac semimetal Cd_3As_2," Nat. Commun. **8**, 2274 (2017).

[25] T. Schumann, L. Galletti, D. A. Kealhofer, H. Kim, M. Goyal, and S. Stemmer, "Observation of the quantum Hall effect in confined films of the three-dimensional Dirac semimetal Cd_3As_2," Phys. Rev. Lett. **120**, 016801 (2018).

[26] C. Zhang, A. Narayan, S. Lu, J. Zhang, H. Zhang, Z. Ni, X. Yuan, Y. Liu, J.-H. Park, E. Zhang, et al., "Evolution of Weyl orbit and quantum Hall effect in Dirac semimetal Cd_3As_2," Nat. Commun. **8**, 1272 (2017).

[27] L. Galletti, T. Schumann, O. F. Shoron, M. Goyal, D. A. Kealhofer, H. Kim, and S. Stemmer, "Two-dimensional Dirac fermions in thin films of Cd_3As_2," Phys. Rev. B **97**, 115132 (2018).

[28] S. Wei, J. Lu, W. Yu, H. Zhang, and Y. Qian, "Isostructural Cd_3E_2 (E = P, As) microcrystals prepared via a hydrothermal route," Crystal Growth & Design **6**, 849 (2006).

[29] P. Cheng, C. Zhang, Y. Liu, X. Yuan, F. Song, Q. Sun, P. Zhou, D. W. Zhang, and F. Xiu, "Thickness-dependent quantum oscillations in Cd_3As_2 thin films," New J. Phys. **18**, 083003 (2016).

[30] E. Arushanov, "Crystal growth and characterization of II_3V_2 compounds," Progress in Crystal Growth and Characterization of Materials **3**, 211 (1981).

[31] A. Pietraszko and K. Lukaszewicz, "Thermal expansion and phase transitions of Cd_3As_2 and Zn_3As_2," Phys. Stat. Sol. A **18**, 723 (1973).

[32] J. R. Clement, "The atomic heat and critical magnetic field of superconducting cadmium," Phys. Rev. **92**, 1578 (1953).

[33] B. B. Goodman and E. Mendoza, "LXII. The critical magnetic fields of aluminium, cadmium, gallium and zinc," Phil. Mag. **42**, 594 (1951).

[34] R. Yan, G. Khalsa, S. Vishwanath, Y. Han, J. Wright, S. Rouvimov, D. S. Katzer, N. Nepal, B. P. Downey, D. A. Muller, et al., "GaN/NbN epitaxial semiconductor/superconductor heterostructures," Nature **555**, 183 (2018).

[35] K. L. Chopra, *Thin film phenomena* (Robert E. Krieger Publishing, Malabar, 1979), ISBN 9780882757469.

[36] E. A. Shapoval, "Critical fields of thin superconducting films," Sov. Phys. JETP **22**, 647 (1966).

[37] E. Z. Kuchinskii, N. A. Kuleeva, and M. V. Sadovskii, "Temperature dependence of the upper critical field in disordered Hubbard model with attraction," J. Exp. Theor. Phys. **125**, 1127 (2017).

[38] K. Kirshenbaum, P. S. Syers, A. P. Hope, N. P. Butch, J. R. Jeffries, S. T. Weir, J. J. Hamlin, M. B. Maple, Y. K. Vohra, and J. Paglione, "Pressure-Induced Unconventional Superconducting Phase in the Topological Insulator Bi_2Se_3," Phys. Rev. Lett. **111**, 087001 (2013).

[39] P. P. Kong, J. L. Zhang, S. J. Zhang, J. Zhu, Q. Q. Liu, R. C. Yu, Z. Fang, C. Q. Jin, W. G. Yang, X. H. Yu, et al., "Superconductivity of the topological insulator Bi_2Se_3 at high pressure," J. Phys.: Condens. Matter **25**, 362204 (2013).

[40] S. Nishihaya, M. Uchida, Y. Nakazawa, K. Akiba, M. Kriener, Y. Kozuka, A. Miyake, Y. Taguchi, M. Tokunaga, and M. Kawasaki, "Negative magnetoresistance suppressed through a topological phase transition in $(Cd_{1-x}Zn_x)_3As_2$ thin films," Phys. Rev. B **97**, 245103 (2018).

[41] I. S. Grigoriev, E. Z. Meilikhov, and A. Radzig, *Handbook of Physical Quantities* (CRC Press, Boca Raton, 1997).

[42] S. I. Novikova, *Thermal expansion of solids* (Nauka, Moscow, 1974).

[43] O. O. Shvetsov, V. D. Esin, A. V. Timonina, N. N. Kolesnikov, and E. V. Deviatov, "Surface superconductivity in a three-dimensional Cd_3As_2 semimetal," ArXiv e-prints (2018), 1811.02475.